Journal of Hazardous Materials 187 (2011) 534–543

Contents lists available at ScienceDirect

Journal of Hazardous Materials

journal homepage: www.elsevier.com/locate/jhazmat

Mineralogical characterization of municipal solid waste incineration bottom ash with an emphasis on heavy metal-bearing phases

Yunmei Wei[a,*], Takayuki Shimaoka[b], Amirhomayoun Saffarzadeh[b], Fumitake Takahashi[b]

[a] Graduate School of Engineering, Kyushu University, 744, Motooka, Nishi-ku, Fukuoka 819-0395, Japan
[b] Department of Urban and Environmental Engineering, Graduate School of Engineering, Kyushu University, 744, Motooka, Nishi-ku, Fukuoka 819-0395, Japan

ARTICLE INFO

Article history:
Received 9 September 2010
Received in revised form 14 January 2011
Accepted 16 January 2011
Available online 22 January 2011

Keywords:
MSWI bottom ash
Glass
Minerals
Heavy metals
Microanalysis

ABSTRACT

Municipal solid waste incineration (MSWI) bottom ash contains a considerable amount of heavy metals. The occurrence and uneven distribution of these heavy metals in bottom ash can increase the complexity of such residues in terms of long-term behavior upon landfilling or recycling. Bottom ashes sampled from three stoker-type incinerators in Japan were analyzed in this paper. This study presents detailed information on the mineralogical characterization of bottom ash constituents and the weathering behavior of these constituents by means of optical microscopy and scanning electron microscopy. It was revealed that bottom ash mainly consists of assorted silicate-based glass phases (48–54 wt% of ash) and mineral phases including melilites, pseudowollastonite, spinels, and metallic inclusions (Fe–P, Fe–S, Fe–Cu, Cu–Sn, Cu–Zn, Cu–S, and Cu–Pb dominated phases), as melt products formed during the incineration process. The compounds embedded in the glass matrix, e.g. spinels and metallic inclusions, played the most important role in concentration of heavy metals (Pb, Zn, Cu, Cr, Mn, Ni, etc.). Other phases such as refractory minerals and ceramics, frequently found in ash, were of less significance in terms of their influence on the involvement of heavy metals. Analysis of lab-scale artificially weathered and 10-year landfilled bottom ash samples revealed that secondary mineralization/alteration of the bottom ash constituents principally carbonation and glass evolution substantially decreased the potential risk of the heavy metals to the surrounding environment.

© 2011 Elsevier B.V. All rights reserved.

1. Introduction

Approximately 77% of municipal solid waste (MSW) is incinerated in Japan, and the generated residue accounts for nearly 64% of all waste disposed in landfill sites (Ministry of Environment of Japan, 2007). The incineration process can reduce the weight of raw waste by up to about 80 wt%, and simultaneously results in high concentrations of heavy metals such as Pb, Cu, and Zn, which could be as much as five times that in raw waste. In recent years, strict attention has been paid to the potential impact of incineration residue on the surrounding environment. Various leaching tests (including up-flow column leaching test CEN/TS 14405, pH dependence leaching test CEN/TS 14429, availability leaching test JLT19, etc.) are commonly used to estimate the mobilization behavior of pollutants in MSWI residue, followed by geochemical simulations based on mineral dissolution/precipitation, adsorption/precipitation or complexation with organic materials [1–5]. However, the simulation is only based on the pH variation without considering the evolutionary process of the bottom ash constituents.

MSWI bottom ash has been reported as being a complex inorganic assemblage mainly composed of fine materials, melt components, small quantities of metallic components, synthetic ceramics and stones, as well as unburned organic matter [1,6–12]. Several complex silicates and oxides exist as primary melt components in bottom ash products, the characterization of which remain undetermined [13]. Due to the multi-component, partially amorphous characteristics of the bottom ash, combinatorial research methods including bulk analysis methods and microanalysis hold the promise of a more profound understanding of the primary and secondary phases in bottom ash. Heavy metals – the focal point of our research – are incorporated into these melt components (glass and minerals) that may undergo mineralogical changes when exposed to the environment. However, only a few studies have focused on the identification and characterization of heavy metal-bearing phases as well as the weathering behavior of such phases. This research work principally studied bottom ash samples from three stoker-type solid waste incinerators located in Fukuoka City,

Abbreviations: MSWI, municipal solid waste incineration; SEM/EDX, scanning electron microscope/energy dispersive X-ray spectroscopy; PPL, plane polarized light; XPL, cross polarized light; RL, reflected light; BSE, backscattered electron; XRF, X-ray fluorescence; XRD, X-ray diffraction.

* Corresponding author. Tel.: +81 928023431; fax: +81 928023432.
E-mail addresses: wei@doc.kyushu-u.ac.jp, ameiwei@msn.com (Y. Wei).

0304-3894/$ – see front matter © 2011 Elsevier B.V. All rights reserved.
doi:10.1016/j.jhazmat.2011.01.070

Japan. The core objectives of these studies are therefore to concentrate on the characterization of various phases in MSWI bottom ash – particularly the heavy metal-bearing phases – by placing emphasis on the spatial distribution and chemical compositions by microanalysis. We have also provided an insight into the relation between the mobilization of heavy metals and the newly formed secondary phases in weathered bottom ashes as a key solution for the long-term behavior of the metallic pollutants.

2. Materials and analytical methods

Freshly quenched MSWI bottom ash was collected from three typical municipal incineration facilities: R, S, and F incineration facility during fiscal year 2004–2009. The incineration temperatures were above 850 °C for all the incinerators. For each plant, about 100 kg of bottom ash was collected from the ash pit by a bucket crane. During sampling, the ash was screened to remove large incombustible and unburned items such as fabric, cans, wood, rubber, ceramics, bricks, and metallic items, which account for less than 5 wt% of all ash materials. The screened ash materials were stored in plastic bags for further laboratory treatment and use (drying, particle selecting, and milling). The MSWI bottom ash from S incineration facility was artificially weathered at elevated environment conditions (temperature: 65 °C; water content: 5–30 wt% by adding water once a week) to accelerate the weathering process. Periodically, subsamples were taken for the sake of determining the leaching concentration of heavy metals by performing a standard Japanese Leaching Test 46 (liquid/solid: 500 ml distilled water:50 g ash; agitation: horizontal shaking at 200 time/m by a reciprocator; time, 6 h; filtration: 0.45 μm organic membrane filter) [14]. The mineralogical alteration phenomenon was concurrently studied. In addition, naturally weathered bottom ash (10 years disposal) from a typical monolayer landfill site was also collected for effective identification of the weathering phenomenon.

Analysis of the intact ash particles is the major focus of this study. Polished thin sections of intact ash particles were prepared according to the conventional method. The prepared thin sections of ash are primarily subjected to identification of the various phases. This is achieved using a petrographic polarized microscope (BX51-33MB, OLYMPUS) in different optical modes (PPL, XPL, and RL). The chemical compositions of each phase, with an emphasis on the heavy metal-bearing phases, were determined by a scanning electron microscope/energy dispersive X-ray spectroscopy (SEM/EDX) with an acceleration voltage of 15–20 kV. Bulk chemical composition was completed by means of acid digestion of the solid samples, and the digested solutions were subjected to inductively coupled plasma optical emission spectroscopy (ICP-OES) and inductively coupled plasma mass spectroscopy (ICP-MS) for determination of dissolved major and minor cations, subjected to chromatography (IC) for analysis of the dissolved anions (P, Cl, and S). The content of silica was measured by X-ray fluorescence spectrometer (XRF). The content of carbon was determined by a solid total organic carbon (TOC) analyzer. X-ray diffraction (XRD) analysis was applied for bulk mineral detection using Cu Kα radiation at a voltage of 30 kV and a current of 40 mA.

3. Results

3.1. Characterization of fresh bottom ash

3.1.1. Chemical composition

The bulk chemical composition of bottom ash (see Table 1) revealed that the incineration products were silicate-based materials with various amounts of other elements. SiO_2, CaO, Al_2O_3, FeO, MgO, Na_2O, K_2O, and TiO_2 were the dominating components, while minor and trace components, such as P, Cl, S, Pb, Zn, Cu, Mn, Ni, and Cr, also exist in different proportions in the bottom ash. Note that the data in Table 1 has been normalized to a hundred percent except for the data below the detection limit. In comparison of the bottom ash from different incinerators, a relatively similar trend generally exists among the contents of the samples. Two times sampling from the same incinerator (Column S-08 and S-09 in Table 1) revealed that, in addition to the incineration system design, input waste composition and seasonal variation may also lead to certain fluctuations from the mean values for each incineration plant.

Table 1
Bulk chemical composition of MSWI bottom ash from different incineration facilities.

Major/minor composition (wt%)	MSWI bottom ash samples			
	R-04	S-08	S-09	F-09
SiO_2 (IV)	31.93	43.69	37.25	36.49
Al_2O_3	16.65	14.03	15.00	14.48
Fe_2O_3 (III)	5.97	6.21	5.16	7.89
TiO_2 (IV)	1.45	1.51	1.63	1.63
MnO (II)	0.08	0.08	0.09	0.10
P_2O_5 (V)	0.02	<0.01	<0.01	<0.01
CaO	33.40	24.67	31.33	28.50
MgO	3.33	2.18	2.58	2.71
Na_2O	2.53	2.46	2.31	2.53
K_2O	0.85	1.50	1.01	0.99
C	2.22	2.16	1.72	2.53
Cl	1.08	1.27	1.57	1.80
S	0.40	0.21	0.35	0.32
Trace composition (mg/kg)				
Zn	3193	3098	3295	3253
Cu	2321	2288	1710	2481
Pb	687	1149	1079	698
Cr	393	158	441	363
Ni	105	79	133	119
Ba	1126	942	835	904
Sb	4	5	4	4
Sn	111	81	64	13
Sr	271	276	362	319
As	<1	<1	<1	<1
Zr	<5	<5	<5	<5
V	1	2	3	2
Cd	1	<1	<1	1
Co	5	8	7	9

3.1.2. Petrographic and chemical analysis of various phases

3.1.2.1. Glass phase. The glass phases are generally regarded as the principal incineration products of MSWI bottom ash. This study adopted the methodology proposed by Font et al. [15] for calculation of the glass content in MSWI bottom ash samples. This method is based on the XRD analysis patterns of mixed bottom ash and standard glass. The glass content of each mixture can be calculated by obtaining the net area between 20° and 40° 2θ of the broad peak of the amorphous components by subtracting the sum area of the whole mineral phases from the total bulk area of the XRD pattern in the 20° and 40° 2θ range with XRD analysis software JADE 6.1. MSW molten slag (more than 99 wt% of glass) from a typical high temperature combustion chamber (HTCC) was collected and utilized as standard glass added into the bottom ash samples at percentages of 50 wt%, 65 wt%, 75 wt%, and 90 wt%. Detailed description of the HTCC facility has been published in a previous paper [16]. The glass content of the MSWI bottom ash samples were finally obtained based on the correction line between % of bulk amorphous (Y) and addition dosage of standard glass (X). Detailed calculation process and results were listed in Table 2. It was seen that the glass content normally account for approximately 50 wt% in the bottom ash with slight deviations among the samples of different sources.

Based on the microanalysis by optical and electronic microscopies, the glass phases in bottom ash can generally be divided

Table 2
Addition dosages of standard glass, total bulk area, mineral bulk area, amorphous bulk area, % of bulk amorphous, and finally obtained values of glass % for bottom ash samples R-04, S-08, S-09, and F-09.

Sample	Added standard glass (wt%)	Bottom ash (wt%)	Total bulk area	Sum mineral area	Amorphous bulk area	Bulk amorphous (%)	$Y-X$	Glass (wt%)
	X	$100-X$	T	M	$T-M$	$Y=100(T-M)/T$	$Y=aX+b$	$-b/a$
R-04	50	50	218,156	50,460	167,696	76.87	$Y=2.2119X-120.31$ ($R^2=0.9991$)	54.39
	65	35	202,911	32,869	170,072	83.81		
	75	25	188,949	21,530	167,419	88.60		
	90	10	180,959	9,280	171,679	94.87		
S-08	50	50	166,061	46,623	119,438	71.92	$Y=2.059X-98.861$ ($R^2=0.9954$)	48.02
	65	35	219,947	43,086	176,861	80.41		
	75	25	191,682	30,301	161,381	84.19		
	90	10	194,344	16,472	177,872	91.52		
S-09	50	50	240,228	55,664	184,564	76.83	$Y=2.188X-117.84$ ($R^2=0.9968$)	53.86
	65	35	197,930	32,009	165,921	83.83		
	75	25	199,220	24,946	174,274	87.48		
	90	10	183,987	8,693	175,294	95.28		
F-09	50	50	187,976	45,467	142,509	75.81	$Y=1.9505X-98.509$ ($R^2=0.9862$)	50.51
	65	35	195,073	28,847	166,226	85.21		
	75	25	200,354	24,204	176,150	87.92		
	90	10	208,590	7,047	201,543	96.62		

into: (1) *melt glass* formed during combustion in the furnace and (2) *waste stream glass*. The latter is usually categorized as refractory (residual) components [10,11,13] that survived incineration as remnants of waste glass input. The melt glass phases are the main melting products of ash under high temperature and complex incineration conditions, which serve as a matrix for bottom ash particles [5,7]. Optical and electron microscopy analysis reveals the following characteristics of the melt glass phases: (a) isotrope, transparent or translucent locally shifting to brown, light blue, green and red colors as observed by plane polarized light (PPL) with respect to its chemical composition, (b) having peculiar banding due to the existence of minute metallic inclusions, (c) highly vesicular due to the entrapment of air and gas bubbles, and (d) coexistence of various well-formed mineral species, quench crystallites and refractory components. Waste stream glass is typically isotropic, presenting a more uniform appearance with few or no vesicles, without a banding feature, and usually only the surface has been partially melted during the combustion process.

Fig. 1 shows a representative melt glass phase with vesicular texture, visible streaks and a slight blue color. Opaque metallic phases (in the center and the top right corner) and fractured quartz fragments exist as remnants of waste input, and a great portion of these waste remnants were set into the glass matrix during combustion. Vesicles of various sizes are easily visible under the PPL mode of optical microscopy. SEM/EDX analysis of representative melt glass phases from different incineration facilities (see Table 3) revealed that the melt glass in bottom ash is chemically heterogeneous with different proportions of major and minor components. The main compositions of melt glass phases from R, S, and F incineration facilities suggest an extreme resemblance in compositional properties. It is understood that silicon, aluminum, calcium as well as some alkali and alkaline-earth elements are the main components of the melt glass. Waste stream glass represents a distinct property as it is quite homogeneous in terms of chemical compositions, containing higher silica and alkali (principally Na) contents, and lower aluminum and calcium contents than the melt glass from the three incineration plants (see Table 3).

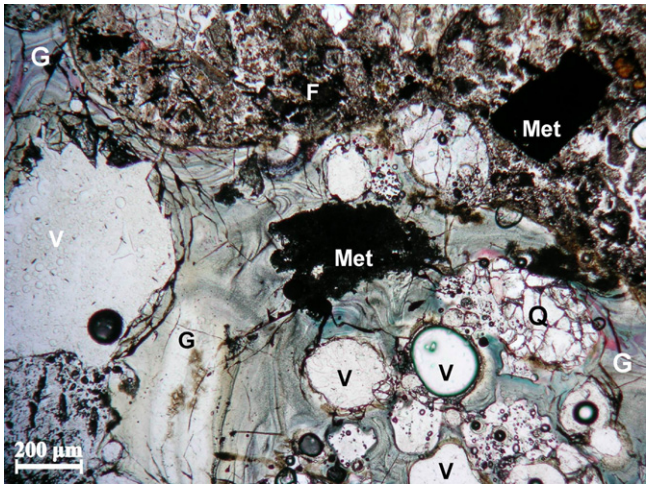

Fig. 1. Photomicrograph of representative melt glass phases under PPL (G: glass; V: vesicle; Q: quartz; Met: metallic; F: fragile).

3.1.2.2. Silicate mineral phase. Melilites, with a general chemical formula of $(CaNa)_2(AlMgFe^{2+})[(AlSi)SiO_7]$, are typical high-temperature products of metamorphosed impure limestone and basic alkaline volcanic. Moreover, melilites were detected to be common constituents of MSW slag at melting temperatures of 1150–1400 °C [17]. Comprehensive microscopy observations of thin sections indicate that melilites are one of the most abundant silicate-based melt minerals in bottom ash, consisting of a series of solid solutions of end members, of which the most important are gehlenite and akermanite. The widespread existence of melilites was also proved through analysis of numerous bottom ash samples by XRD in this study. The melilites found in the bottom ash used in this study usually exist as crystal aggregates embedding in glass matrix, characterized by subhedral to euhedral microphenocrysts, as shown in Fig. 2a. Optical observation and compositional analysis by SEM/EDX indicate that the melilites usually have a similar chemical composition as the melt glass matrix, and that the entrapping of melilites makes the melt glass easily distinguishable from the waste stream glass.

Pseudowollastonite ($CaSiO_3$) is another silicate-based melt product of incineration, detected as radiating and fibrous aggregates (Fig. 2b). Pseudowollastonite was reported as high-temperature outcome >1125 °C that occurs in slag, cement and ceramics [17]. The detection of pseudowollastonite in the bottom ash samples used in this study indicates the existence of higher temperature spots (>1125 °C) in the incineration furnaces. Quantitative analysis by electron microscopy reveals that the pseudowollastonite in bottom ash contains a small amount of sodium, aluminum and magnesium as additional substituent to calcium and silicon. A rough stoichiometric formula was estimated

Table 3
Chemical compositions of melted glass phases from R, S and F incineration facilities; waste stream glass is listed as a reference.

Composition (wt%)	R-04													
	R2_24-1	R2_25-1	R2_21-3	R3_210-1	R3_24-1	R3_21-4	R3_214-1	R3_215-3	R3_27-1	R3_28-1	R3_22-1	R3_25-4	R2_21-12	Average
Na_2O	3.02	3.63	3.89	4.77	4.81	4.55	4.27	7.38	6.30	5.61	8.01	9.78	3.59	5.35
MgO	0.94	8.23	1.03	5.04	5.21	4.95	9.61	2.51	3.43	2.64	2.89	4.78	–	4.27
Al_2O_3	10.57	21.46	20.40	30.20	23.18	22.45	19.62	15.84	14.80	13.48	20.81	14.05	18.87	18.90
SiO	30.84	34.96	36.15	38.32	39.48	44.45	45.90	46.69	48.43	50.80	52.29	59.04	60.94	45.25
P_2O_5	2.09	1.10	0.81	–	1.94	0.59	1.79	1.43	0.95	1.11	1.21	–	–	1.30
K_2O	0.70	0.81	0.56	1.20	1.54	1.45	1.65	1.41	2.05	2.24	3.48	3.86	2.35	1.79
CaO	29.36	20.55	21.93	17.50	19.77	18.48	14.87	19.45	13.68	12.11	6.19	5.68	2.82	15.57
TiO	1.58	2.53	1.09	1.87	1.51	2.31	0.72	1.53	3.03	5.27	3.46	0.40	0.32	1.97
FeO	19.84	5.66	12.67	0.76	1.99	0.14	1.25	3.72	6.31	5.84	3.46	1.44	9.87	5.61
CuO	0.27	0.26	0.68	0.08	0.12	0.14	0.06	–	0.22	0.18	0.00	0.97	0.43	0.28
ZnO	0.18	0.25	0.09	0.00	0.23	0.22	0.11	–	0.40	0.33	0.08	–	0.37	0.21

Composition (wt%)	S-08and S-09									F-09				Waste glass
	S3_2-2	S7_11-1	S7_12_4	S5_27_3	S5_27_3	S5_21_2	S7_1-4	S5_23_1	Average	Fl_1-2	F2_1_2	F2_2_3	Average	W-1
Na_2O	5.25	3.79	2.45	4.14	4.14	2.80	3.17	3.22	3.62	2.45	5.54	8.59	5.53	12.91
MgO	6.19	3.27	1.88	3.69	3.69	3.05	6.17	2.33	3.78	0.95	2.40	1.49	1.61	–
Al_2O_3	17.58	16.78	9.31	26.42	27.42	15.31	15.65	20.29	18.60	27.91	13.06	8.20	16.39	2.87
SiO	32.09	38.44	40.79	41.08	41.58	50.06	51.48	53.77	43.66	37.25	46.89	57.03	47.06	72.63
P_2O_5	5.18	6.31	–	1.52	–	0.67	0.35	–	2.81	–	–	–	1.50	1.50	–
K_2O	1.26	1.79	1.16	1.43	1.43	0.00	3.24	1.67	1.50	1.31	4.44	2.52	2.76	1.33
CaO	21.48	18.67	21.25	21.29	21.29	24.21	7.07	14.68	18.74	20.44	18.43	9.44	16.10	10.24
TiO_2	2.65	2.23	0.00	–	–	1.00	3.21	–	1.82	8.88	2.09	–	5.49	–
FeO	7.50	6.94	22.04	0.28	0.28	1.61	7.07	2.10	5.98	0.78	6.64	7.35	4.92	–
CuO	0.12	0.38	0.27	–	–	0.22	–	0.33	0.26	–	–	–	–	–
ZnO	0.44	0.99	0.31	–	–	0.51	–	0.63	0.58	–	0.58	–	0.58	–

to be $(Ca_{0.48–0.69}Na_{0.06–0.21}Mg_{0–0.18})(Si_{0.84–0.97}Al_{0.03–0.18})O_3$, which implies undersaturation of cations, such as Ca, Na, and Mg. It should be noted that the pseudowollastonite shows a preference for embedding in high-silicon glass, and because the mandated temperature for MSWI furnaces in Japan is above 850 °C, the pseudowollastonite might not often be detected in bottom ash.

3.1.2.3. Non-silicate mineral phase. The general chemical formula of spinel group minerals is $A^{2+}B_2{}^{3+}O_3$, where A^{2+} represents a metal having a valence of plus two (commonly Fe^{2+}, Mg^{2+}, Zn^{2+}, Mn^{2+}, Ni^{2+}, and in rare cases Cu^{2+}, Pb^{2+}, Co^{2+}, Cd^{2+}), and B represent metals having a valence of plus three (Al^{3+}, Fe^{3+}, Cr^{3+}, and sometimes Ti^{4+}). Optical microscopy and SEM/EDX analysis disclose that MSWI bottom ash contains a considerable amount of spinels group minerals, which show a preference for embedding in melt glass as aggregates.

Magnetite (Fe_3O_4) is one of the end-member spinel group minerals. The typical chemical composition of Sample 1 in Table 4 is of a material close to the theoretical composition of magnetite. Although in nature the continuous substitution of Fe^{3+} by Al^{3+} to hercynite ($FeAl_2O_4$) does not seem to appear, the existence of a Fe_3O_4–$FeAl_2O_4$ system was demonstrated experimentally at temperatures above 858 °C [18]. As a high-temperature melting product, some intermediate varieties between magnetite and hercynite were also detected for bottom ash as shown in Sample 2 and Sample 3 in Table 4. Partial substitution of Fe^{2+} by Mg^{2+}, Ca^{2+} and Mn^{2+}, substitution of Fe^{3+} or Al^{3+} by Si^{4+} and Cr^{3+} occurred as proved by Sample 3 in Table 4. Magnetite and Al-substituted varieties are the most common spinel group minerals in bottom ash, characterized by rectangular, triangular, or toothed crystal shapes (see Fig. 3).

Fe–Ti dominating spinels are another group of spinels in bottom ash samples, as specified by Sample 4 and Sample 5 in Table 4. Despite the complex chemical composition of Fe–Ti spinels in Sample 4 of Table 4, a euhedral crystal shape still can be identified,

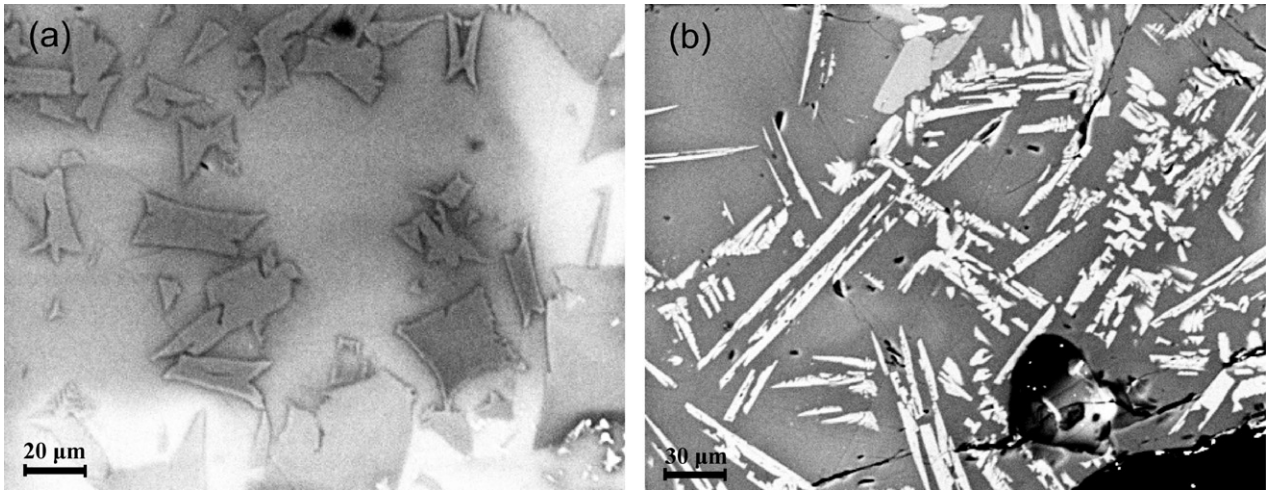

Fig. 2. BSE image of melilite (a) and (b) pseudowollastonite.

Table 4
Representative chemical compositions of spinels identified by SEM/EDX.

Elements (wt%)	Points of analysis				
	1	2	3	4	5
	Fe–Fe	Fe–Al	Fe–Al–Cr	Fe–Ti	Fe–Ti–Cr–Pb
SiO_2	–	–	7.90	8.20	11.00
CaO	–	–	2.83	6.97	5.33
FeO	96.54	64.35	61.97	40.74	16.04
TiO_2	–	–	0.39	18.17	34.04
Al_2O_3	1.02	32.04	15.03	11.84	2.49
MgO	2.16	3.30	2.72	8.43	3.40
MnO	0.15	0.13	2.15	0.74	0.27
PbO	–	–	–	–	7.56
ZnO	–	0.46	0.51	2.02	0.56
CuO	–	–	–	1.58	0.47
Cr_2O_3	0.11	0.23	6.41	1.33	19.41
Total	99.98	100.51	99.91	100.02	100.57

All iron (Fe^{2+} and Fe^{3+}) in the spinels is expressed as a divalent oxide FeO.

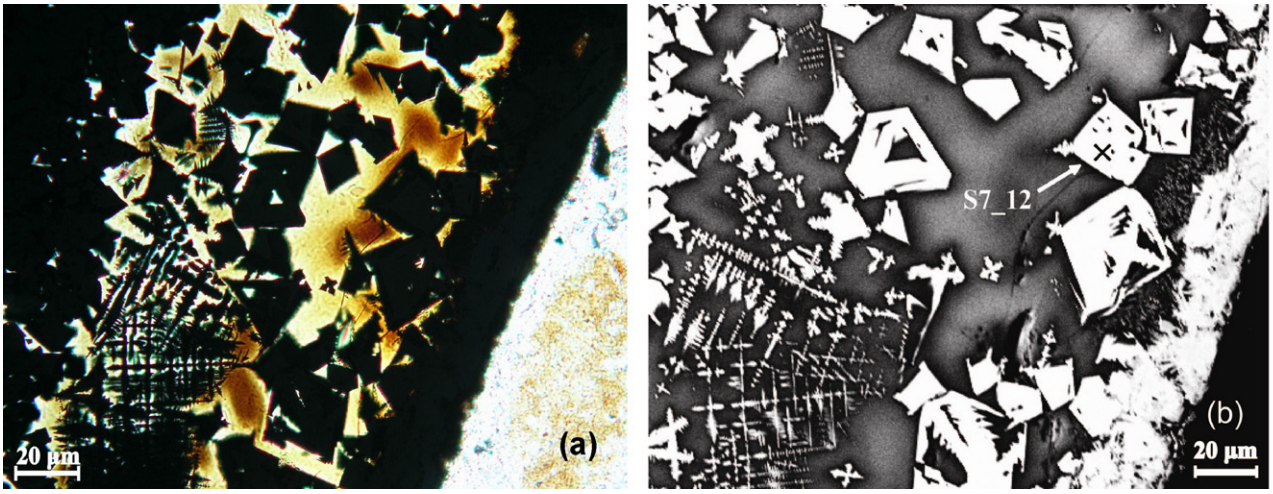

Fig. 3. Photomicrograph of spinels under PPL (a) and BSE image of the same panel (b).

similar to that of the magnetite in Fig. 3. The Fe–Ti–Pb–Cr spinels in Sample 5 of Table 4 are much more complex in chemical composition as a result of the incorporation of Pb^{2+}, Mg^{2+}, Zn^{2+}, Mn^{2+} and Cu^{2+}, as well as Cr^{3+} and Al^{3+}. The crystal face of the Fe–Ti–Pb–Cr spinels is quite different from that shown in Fig. 3, characterized by a smaller crystal size, acicular and elongated crystal shapes.

In addition to spinels, metallic inclusions are another group of minerals encapsulated in the melt glass matrix. Most of the metallic inclusions have sizes ranging from one micron (or even less) to hundreds of microns with spherical or subspherical shapes, existing as single inclusion or clustered aggregates (Figs. 4 and 5). These metallic inclusions are the most common heavy metal-bearing phases, primarily including Fe–P, Fe–S, Fe–Cu, Cu–Sn, Cu–Zn, Cu–S and Cu–Pb couple-dominated combinations, of which Fe–P alloys account for more than 80% of the existing metallic inclusions. Moreover, complex associations of the above couple-dominated compounds are regular products of the solid waste incineration process. Typical images of the metallic inclusions were collected and shown in the following content in order to exhibit their characteristic properties.

Fig. 4 shows a subspherical particle with compositional zoning characteristics. The chemical composition of each zone was determined by SEM/EDX (see Table 5). Zones 1 and 5 were detected to be compounds rich in Cu and S. Zones 2 and 7 are Fe–P combinations. Zone 3 is chiefly composed of Fe and Cu (collectively more than 85 wt%). Zone 4 is a Cu-dominant compound with a small amount of Fe as an impurity. In the right core area (Zone 6), a substantial increase in Zn (27 wt%) is observed, together with proportions of Cu, Fe and S, as well as trace amounts of Pb and Cd. The brighter dots embedded in the central area were determined to be Pb concentrators (approximately 30 wt% of Pb). Insignificant amounts of Si, Al,

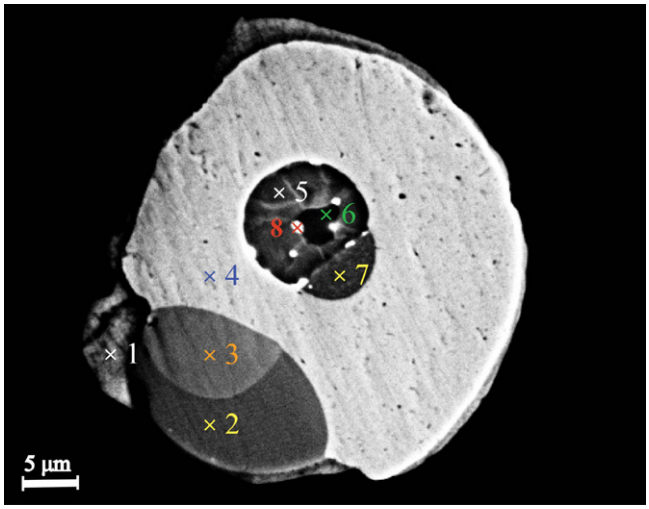

Fig. 4. BSE image of metallic inclusion (Cu–S–Pb–Zn–Fe–P).

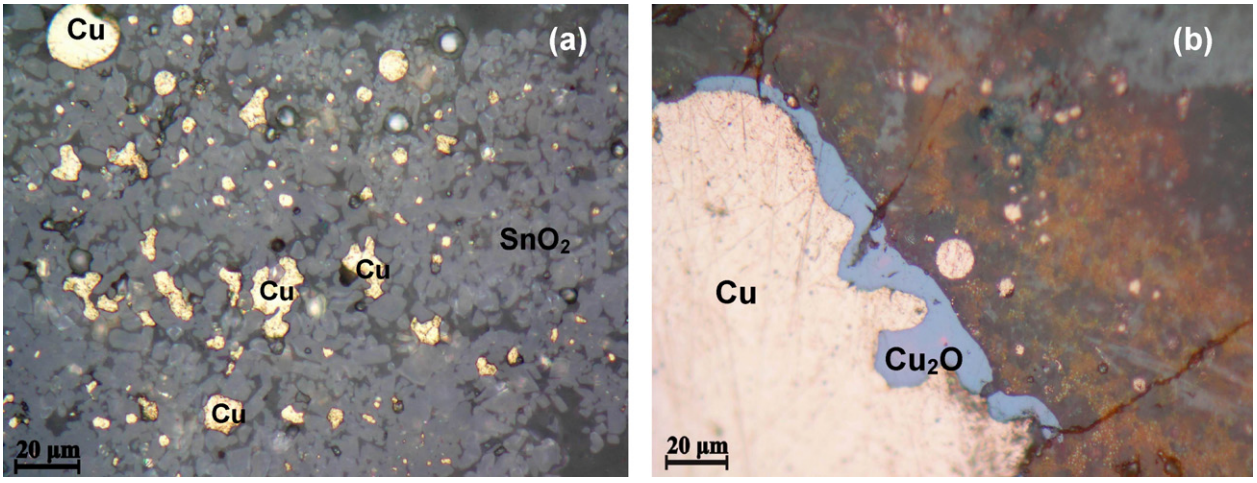

Fig. 5. Photomicrograph of numerous Cu metallic inclusions and tin oxides (a), partial oxidization of the Cu metal (b), both under RL.

Table 5
Chemical compositions of points designated in Fig. 4.

Elements (wt%)	Points of analysis							
	1	2	3	4	5	6	7	8
Cu	55.69	3.80	8.05	79.40	49.60	10.23	5.84	22.36
S	19.74	1.05	–	–	23.21	27.09	0.57	19.09
Fe	7.36	71.22	77.72	3.72	12.16	15.50	69.37	8.61
P	0.74	11.89	1.59	0.23	–	–	12.00	–
Pb	–	–	–	–	–	1.99	–	28.66
Zn	–	–	–	–	–	27.03	–	7.13
Cd	–	–	–	–	–	2.59	–	0.98
Ni	–	0.91	0.64	–	–	–	0.57	–
Total	83.53	88.87	88.00	83.35	84.97	84.43	88.35	86.83

Ca, and Ti, were also detected incorporated into the whole particle. Compositional analysis of the metallic inclusion in Fig. 4 indicates that couples of Fe and P, Cu and S, Fe and Cu have a remarkable affinity with each other.

Combinations of Cu and Sn as well as affiliated metallic inclusions were frequently detected in bottom ash. Fig. 5a shows images of dotted Cu inclusions (83 wt% of Cu) coupled with Sn oxides (SnO_2, involving less than 2 wt% of Cu). It is presumed that it was possibly a piece of Cu–Sn combination that was melted in the incineration furnace on account of its melting point of 700–900 °C. The Cu element congregated forming metallic inclusions, while the Sn was oxidized to SnO_2 due to its low melting temperature. Occasionally, cuprous oxide (Cu_2O) was observed as coating of Cu (see Fig. 5b). No cupric oxide (CuO) was found in this study.

3.1.2.4. Other phases. In addition to the melt glass phase and the various encapsulated compounds (silicate-mineral phase and non-silicate mineral phase), other phases such as calcium-rich mineral phases and refractory phases account for a great proportion of the bottom ash. These phases, not the focus of this study, are included in this paper for a complete understanding of the bottom ash constituents. It is well known that in a MSWI furnace, carbonates are calcined to form lime (CaO). This lime is consequently hydrated to portlandite as a result of an exothermic reaction (1) after immediate contact with water during quenching. Subsequently, the portlandite reacts with CO_2 in air according to reaction (2) [10,19].

$$CaO + H_2O = Ca(OH)_2 \quad \Delta H = -65\,kJ/mol \tag{1}$$

$$Ca(OH)_2 + CO_2 = CaCO_3 \quad \Delta H = -84\,kJ/mol \tag{2}$$

Microscopic observations show the presence of portlandite and calcite in freshly quenched bottom ash (Fig. 6). These photomicrographs show that a dark brown portlandite fragment and anhedral aggregates of calcite are surrounded by non-distinguishable fragile materials as well as refractory materials. The refractory materials are products from the waste stream that survive the solid waste incineration process, consisting of waste glass, minerals, ceramics, and unburned materials. Although frequently found in bottom ash, they are of less significance in terms of their influence on heavy metals. Waste stream glass was introduced together with the melt glass phases in Section 3.1.2.1 for effective discussion. The refractory minerals usually remain intact or only the rim is partially altered, including quartz, K-feldspar, plagioclase, biotite and in rare cases mafic minerals (pyroxene and amphibole) and cordierite. The group of refractory phases, due to their high resistance to extreme conditions (high temperature), basically keep their original chemical compositions (compositions formed in natural conditions) during the combustion process, and the impurity components cannot easily be chemically incorporated into these phases.

3.2. Weathering phenomenon of MSWI bottom ash

3.2.1. Weathering of calcium-rich phase

As a thermodynamically unstable multi-component material, the MSWI bottom ash should undergo evolution immediately after its production. Of all the weathering reactions happened to the bottom ash, alteration of the calcium-rich phases (e.g. carbonation) should govern the initial stage of weathering. In an effort to testify this hypothesis, an accelerated weathering experiment was conducted at elevated experimental conditions. Subsamples of the bottom ash were collected periodically for characterization of the secondary mineralization phenomenon and corresponding mobilization behavior of the heavy metals. For instance, the X-ray powder diffractograms of these subsamples in Fig. 7 indicate a dramatic increase in the amount of calcite as a function of weathering time. Corresponding, these reactions directly resulted in a drop in pH (see Fig. 8a) and subsequently a decline in the leaching concentration of Pb, Zn, and Cu (Fig. 8b), indicative of an affinity between pH and the leaching behavior of the heavy metals. Similar trends for Pb, Zn, and Cu were found by Chimenos et al. [9], who conducted a lab-scale natural weathering experiment in a chamber for three month. Moreover, according to a 10-year investigation of the leachate from a landfill site (composed of 50% MSWI residues and 50% non-combustible materials), Pb and Zn have similar leaching trend with the results from this study [20]. All these results make clear the importance of the initial weathering reactions on stabilization of the heavy metals.

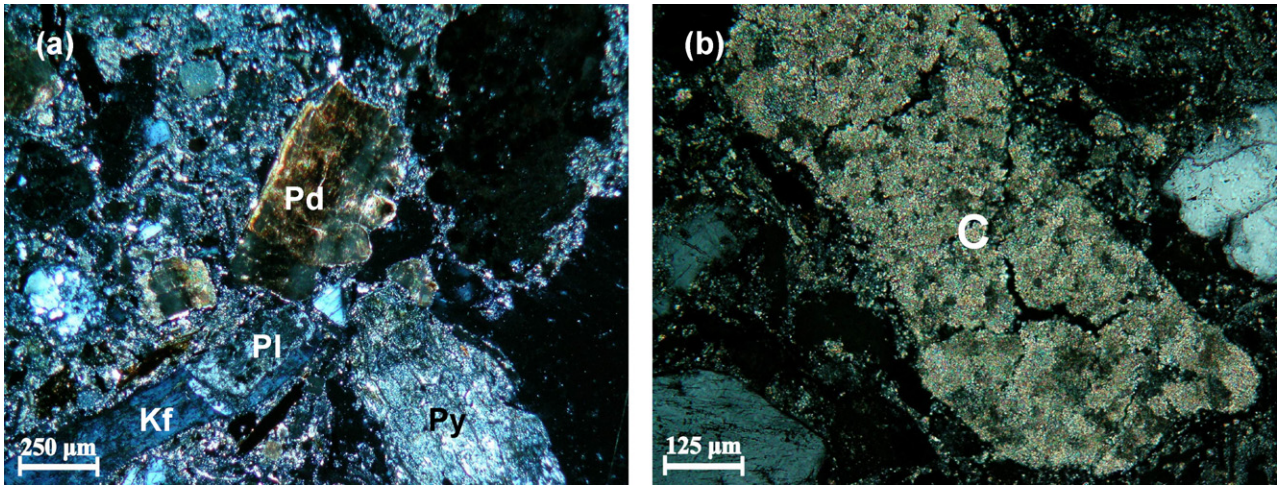

Fig. 6. Photomicrograph of portlandite, plagioclase, K-feldspar, and pyroxene under XPL (a), and calcite crystal under XPL (b) (Pd: portlandite, Pl: plagioclase, Kf: K-feldspar, Py: pyroxene, C, calcite).

3.2.2. *Weathering of silicate-based glass phase*

In an advanced weathering-stage, evolution of other phases (e.g. glass) which are comparatively resistant to the external environmental factors should take place. The silicate-based glass has been determined to be the dominant phase in bottom ash, accounting for approximately 50 wt% of the ash material. Additionally, the glass phase has long been reported as being a metastable material. The specific geochemical conditions of the landfill sites (moderately to highly alkaline) should enhance the evolution process of the glass as well as the encapsulated compounds, resulting in textural and chemical evolutions. However, it should be emphasized that the evolution of the glass phase, not like carbonation, appears to proceed in a slow manner, and the evolution products usually are not well-crystallized phases. These characteristics necessitate the utilization of long-term weathered ash samples and effective analytical methods for studying this weathering phenomenon. Hereby, this research work utilized a 10-year naturally weathered bottom ash sample in an effort to illustrate the alteration phenomenon of glass with respect to the microanalysis results. Fig. 9 shows an example of such evolution phenomenon. It was seen that the primary glass presents more or less uniform morphology regardless of the perfect vertical banding texture (alignments of minute metal-

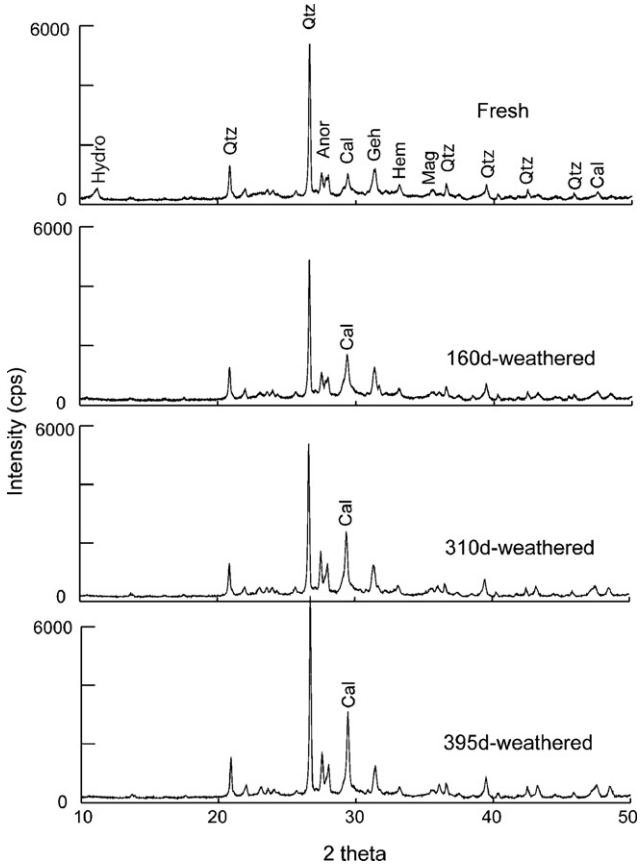

Fig. 7. X-ray diffraction data for MSWI bottom ash samples with weathering time of 0 day, 160 days, 310 days and 395 days. (Hydro, hydrocalumite; Qtz, quartz; Anor, anorthite; Cal, calcite; Geh, gehlenite; Hem, hematite; Mag, magnetite).

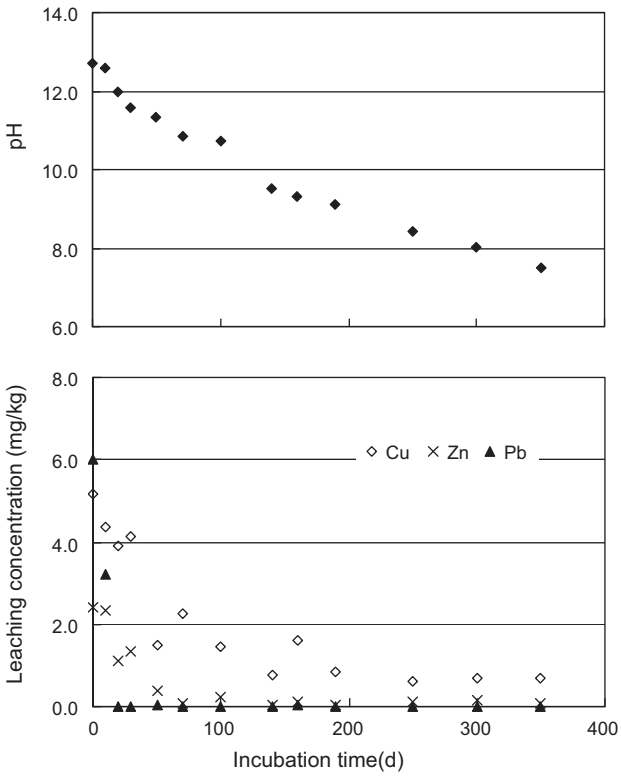

Fig. 8. Variation of pH and leachability of Pb, Zn, and Cu as a function of weathering period.

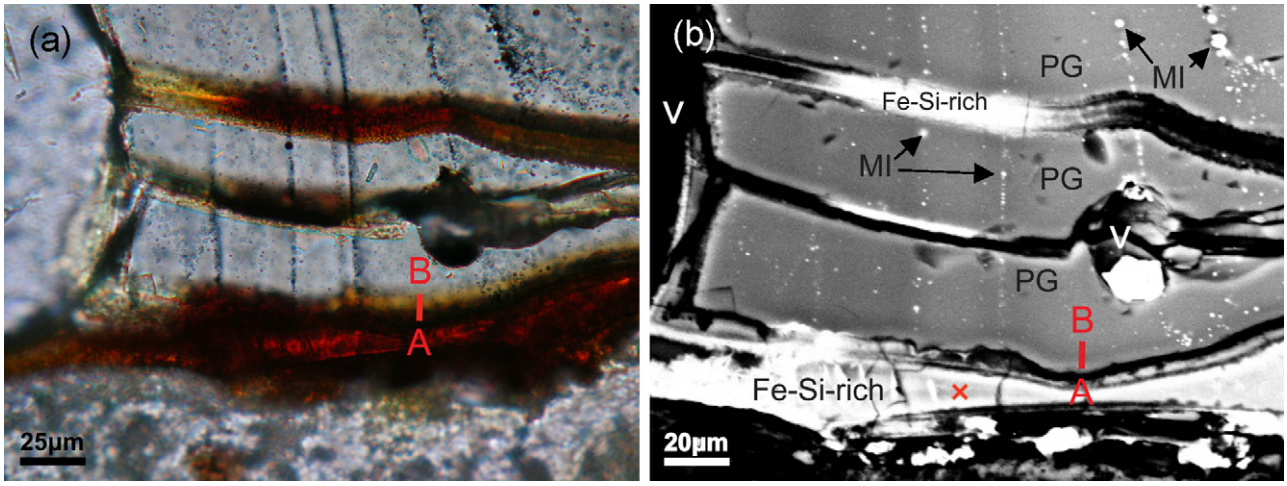

Fig. 9. Photomicrograph (a) and BSE image (b) representing glass evolution process and formation of new precipitate beyond the glass rim and along the walls of the fissures. Compositional analysis of the designated line and point are shown in Fig. 10 (PG: primary glass; MI: metallic inclusion; V: vesicle; Fe–Si-rich: Fe–Si-rich precipitate).

lic inclusions). The fissures in the glass matrix disconnected two pieces of glass apart from the parent material, which provides more accessible channels for the percolated fluid.

The photomicrograph in Fig. 9a shows that the secondary precipitates has a quite different morphology from the primary glass, characterized by a distinctive red-brown color. These precipitates coat on the surface of the glass or infill the fissures within the glass matrix. The results of EDX line-scan of the designated line (from A to B in Fig. 9) disclosed that the soluble elements (Na and Ca) as well as the moderately soluble element (Si) were partially removed from the glass matrix; simultaneously, passive invasion of Fe into the glass happened as being testified by a distinct decreasing trend of Fe (see Fig. 10), numerically from approximately 20 to 10 wt%. The layer, which is characterized by obvious loss of glass elements (Na, Ca, and Si) and in some cases accompanied by simultaneous gain of Fe, is referred to as "leaching layer", namely the alteration front of the glass. The thickness of the leaching layer was detected to range from 2 to 4 μm in this study. Similar alteration phenomenon had been found for igneous glass by Thorseth et al. [21]. Compositional analysis of the amorphous precipitates in Fig. 10b revealed that they were rich in Fe and Si. Certain soluble ions, such as Na, K and Ca, were partially retained in these new phases. Moreover, the new precipitates entrapped a significant amount of heavy metals (3.29 wt% of Pb and 0.91 wt% of Zn).

4. Discussion

This study revealed that glass and non-silicate minerals (spinels and metallic inclusions) were the most important constituents in bottom ash, in consideration of the reutilization or disposal of the bottom ash in a safe manner. The amount of heavy metals in bottom ash was relatively high, and the heavy metals principally concentrated in the non-silicate minerals that preferentially embedded in the glass matrix. Thus, the following discussions mainly focused on the characteristics of the glass and the non-silicate mineral phases as well as the weathering phenomenon of such phases.

It has been outlined that the glass phases are the main constituents of bottom ash (approximately 50 wt%), entrapping assorted mineral phases – either refractory fragments (quartz and plagioclase) or melt clusters (melilites, spinels, and metallic inclusions), and having numerous discrete vesicles and fractures that resulted from rapid quenching. Particularly, the existence of these vesicles and fractures may increase accessibility to water and gas in view of the weathering process of glass. The heterogeneous chemical compositions of the melt glass with respect to its major compositions SiO_2, CaO, Al_2O_3, Na_2O, and K_2O may suggest different weathering patterns (mechanism, weathering product, etc.).

The metals in bottom ash usually exist as various chemical combinations, e.g. several metals generally mixed together, or even with additional nonmetal elements. To gain a clear understanding of the behavior of bottom-ash elements in the high-temperature incineration process, particularly the behaviors of heavy metals, knowledge concerning the igneous process in geochemistry would be most helpful. According to Goldschmidt's classification, the elements in the earth are categorized into four groups: lithophile (Na, K, Al, Si, Ti, P, O, Fe, Mn, Zn, etc.), siderophile (Fe, Ni, Cu, Zn, P, Mn, etc.), chalcophile (Cu, Zn, Pb, S, Fe, Sn, etc.), and atmophile (H, N, and O). Only the elements detected in bottom ash are listed in the parentheses. Lithophile, siderophile and chalcophile refer to the tendency of the element to partition into a silicate, metal, or sulfide liquid, respectively.

Magnetite, as well as a series of Al-substituted and Ti-substituted varieties, is commonly identified in bottom ash. Heavy metals, such as Zn^{2+}, Mn^{2+} and Cr^{3+}, are frequently detected incorporated into these spinels in an inconstant amount. These findings are consistent with the fact that Zn^{2+}, Mn^{2+} and Cr^{3+} have relatively high free energies ($|\Delta G_f^\circ|$) of oxidization, correspondingly 237.9, 281.1 and 362.9 kJ per oxygen atom at 827 °C respectively, indicating their easily oxidable properties [22,23].

Fe–P dominating alloys are the most abundant metallic inclusions in bottom ash, comprising of 60–95 wt% of Fe and P, and usually associate with other minor elements (Si, Ca, Al, Cu, Zn, and Pb). Note that P is concentrated in both the glass phases shown in Table 3 and metallic alloys (Point 2 and Point 7 in Fig. 4), as might be expected from its lithophile and siderophile characteristics [23]. Except for the Fe–P alloys, combinations of Fe and S were frequently detected in bottom ash, which provided sound evidence of the siderophile property of Fe.

Cu and its combinations or compounds are used for kitchen utensils, electrical wire, pigments, catalysts, stabilizers and so on. Due to the comprehensive use of Cu in our daily lives, the Cu concentration in MSWI bottom ash ranges from 1710 to 2481 mg/kg (Table 1). These Cu-rich combinations were melted or partially melted, followed by recomposing, and were finally formed as numerous metallic grains and scattered in bottom ash. In this study, Cu was constantly found as metallic inclusions in thin sections of bottom ash, including element Cu (usually more than 83 wt% of Cu), alloys (5–60 wt% of Cu, mainly Cu–Sn, Cu–Fe, Cu–Zn, and Cu–Pb), sulfide, and in rare cases, lower oxides of Cu (Cu_2O). This is closely related to its strong resistance to oxidation regarding the low

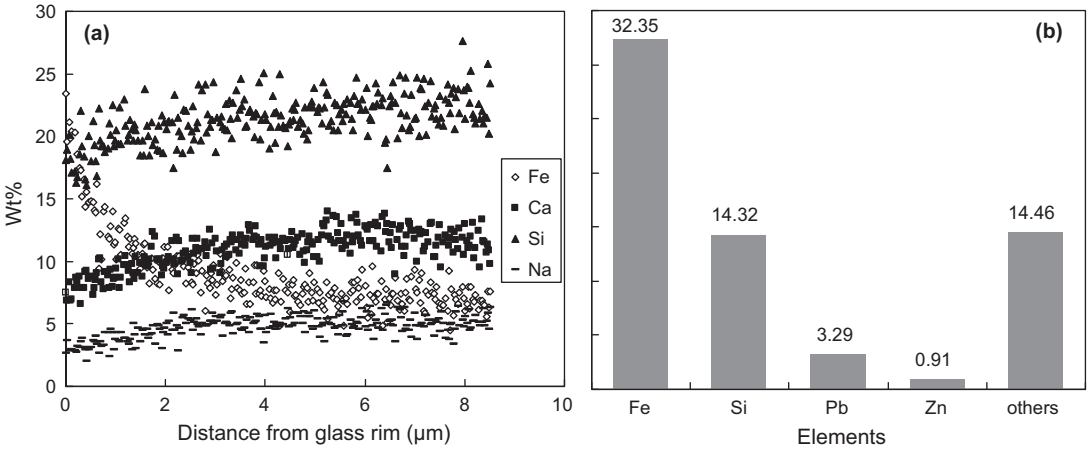

Fig. 10. Alteration patterns of the glass phase with respect to variation of elements Fe, Si, Ca, and Na (a), and point compositional analysis data of the electropositive elements in the new precipitate.

$|\Delta G_f^\circ|$ of oxidization at high temperature [22,23]. Although it was reported that higher oxides of Cu (Cu_2O) were abundant in bottom ash [24], no such minerals were detected in this study. When bottom ash is exposed to the atmosphere (as in landfilling or recycling), further oxidization of Cu metals and their combinations might take place.

Metal Pb and its compounds are mainly used for the production of Pb batteries, solder for electronic devices, paint materials, crystal glass, ink and so on. Pb is of great interest not only because of its economic importance, but also because of its pollution to surrounding environments. From the viewpoint of geochemistry, Pb is chalcophile, and perhaps slightly siderophile [23]. The analysis result of Point 8 in Table 5 ($Pb_{0.28}Cu_{0.22}Fe_{0.08}$) proves the aforementioned properties of Pb. The high affinity of Pb with Fe and Cu was also found in MSW melting slag [25]. Pb cannot be easily incorporated into mineral species in natural systems, which might be ascribed to its large ionic radius (1.26 Å) and charge (plus two valence) [23]. However, MSWI bottom ash was identified as having certain specific behavior, e.g. 7.56 wt% of PbO was incorporated into the spinel crystals (see Table 4). The long-term stability of these specific products should be taken notice of as it might be thermodynamically unstable in natural environmental systems.

A clear understanding of the distribution of the heavy metals is essential for analyzing the fate of them in view of disposal or recycle. Of the entire weathering phenomena in MSWI bottom ash, carbonation and glass alteration are emphasized in this paper in that the corresponding weathering products play an essential role on the behavior of the heavy metals. It has been concluded from Fig. 8 that Pb, Zn, and Cu become more stable as the weathering process proceeds, which should be primarily attributed to the declined pH. Furthermore, the carbonation is generally regarded as a dominant process controlling pH variation especially in the first few decades after disposal. Apart from pH falling due to carbonation, direct involvement of heavy metals (Pb and Zn) by the newly formed carbonates, although reported by Piantone et al. [12] as a result of electron element micro-mapping using electron microscopy, was not detected in this study. Based on these findings, basically it is believed that the existence and evolution of these alkaline minerals could impact the leachability of heavy metals principally by changing the pH, and the direct involvement of heavy metals by them may play a less significant role.

Evolution of the glass phase into a relatively stable phase, although not as rapid as carbonation in the bottom ash, has been identified in 10-year naturally weathered samples in this study. The degree of mobility of the glass elements largely depends upon the pH conditions of the percolated fluid. It has been reported that a pH > 9 is necessary to dissolve the glass network-forming element Si [20]. From this viewpoint the alkaline geochemical condition in the investigated landfill site should be quite favorable for destruction of the glass matrix. Evolution of the glass phases usually result in white "gel" phase, for example, evolution of the igneous glass produces such gel phases [20,26]. However, the new precipitates in Fig. 9 display a red-brown color. This is due to the incorporation of Fe-rich materials, as expected from the fact that in an oxidizing environment at pH over 3, Fe, Ti, and Al will precipitate as oxides/hydroxides [20]. Based on a profound understanding of the glass alteration mechanism, it was perceived that the Fe–Si-rich precipitate in Fig. 9 was a combined product of both glass alteration and dissolution of the Fe-rich metallic inclusions. The strong adsorption capacity of heavy metals by these new precipitates could partially be ascribed to its high porosity as a result of leaching out of easily soluble elements (Na and Ca) from the glass matrix. In addition, the co-precipitated Fe-rich materials (possibly iron hydroxide) should also contribute to adsorption of the heavy metals. Finally, it should be pointed out that, the gel phase is only the early stage product of glass evolution; further evolution of the gel phase to a more stable material (possibly clay material) is expected to take place.

5. Conclusions

This paper studied the properties of MSWI bottom ash from the chemical and mineralogical standpoint, with an emphasis on the distribution patterns of heavy metals as well as the factors that control the mobilization behavior of such heavy metals in the weathering process. Bottom ash is derived from the thermal processing of MSW. Part of the inorganic fraction of the waste turns into melt components (glass and minerals), and part of them survive the thermal processing to form heat-resistant refractory phases. The glass phases are the main constituents, accounting for approximately 50 wt% of bottom ash, with various chemical compositions. Therefore, it is not easy to suggest a uniform alteration manner upon exposure to the environment. However, the compositional values from different incineration plants show a comparative resemblance in their compositional properties, which suggests that high-temperature processing (above 850 °C) of solid waste produces more-or-less uniform outcomes in view of both chemical and mineralogical characteristics. All the melt mineral phases (silicate minerals and non-silicate minerals) as well as part of the refractory phases embed in a melt glass matrix.

It is understood that the incineration process of MSW results in a prominent increase in the amount of heavy metals. Some of them are elements of environment concern, such as Pb, Zn, Cu, Mn, and Cr. Of all the various phases in bottom ash, the non-silicate minerals were detected to be the most significant concentrators of heavy metals. Cr, Zn, and Mn are ubiquitously incorporated into spinels, while Cu and Pb show evidence of opposite behaviors, which are substantially associated with Fe, Sn, and Zn, present as metallic inclusions bound in the silicate glass matrix. The behavior of heavy metals during the incineration process depends on their own physical and chemical properties. The geochemical classification by Goldschmidt presents a good explanation for elements of concern, especially for P, Cu, and Pb. It should be noted that, despite the heterogeneous chemical compositions of the numerous metallic inclusions, most of them were in the metallic state (not oxidized).

Generally, it was concluded that the long-term behavior of the elevated amount of heavy metals depends to a great extent upon the behavior of the host phases, especially the weathering rate and alteration products of the calcium-rich phases and silicate-based glass phases. Of all the factors related with the mobilization behavior of the heavy metals, the carbonation process is of great importance with respect to their dominant role in pH variation especially in the first few decades, in that pH is a key factor that controls the leaching behavior of the heavy metals. In addition to the newly formed carbonates, the glass-derived secondary products also contributed to immobilization of the heavy metals. It was perceived the glass-derived products should play a long-lasting role since evolution of the glass phase proceeds in a relatively slow manner. A clear understanding of the various phases in MSWI bottom ash as well as the possible alternation phenomenon when subjected to weathering is essential for prediction and explanation of the behavior of heavy metals of environment concern.

Acknowledgements

The authors appreciated greatly the financial support from the Grants-in-Aid for cooperative study (approved by H22-Shinene-kan-0401022) of the New Energy and Industrial Technology Development Organization (NEDO).

References

[1] J.A. Meima, R.N.J. Comans, Geochemical modeling of weathering reactions in municipal solid waste incinerator bottom ash, Environ. Sci. Technol. 31 (1997) 1269–1276.
[2] J.A. Meima, R.N.J. Comans, Application of surface complexation/precipitation modeling to contaminant leaching from weathered municipal solid waste incinerator bottom ash, Environ. Sci. Technol. 32 (1998) 688–693.
[3] J.A. Meima, R.N.J. Comans, The leaching of trace elements from municipal solid incinerator bottom ash at different stages of weathering, Appl. Geochem. 14 (1999) 159–171.
[4] J.J. Dijkstra, H.A. Van Der Sloot, R.N.J. Comans, The leaching of major and trace elements from MSWI bottom ash as a function of pH and time, Appl. Geochem. 21 (2006) 335–351.
[5] T. Shimaoka, R.N. Zhang, K. Watanabe, Alterations of municipal solid waste incineration residuals in a landfill, Waste Manage. 27 (2007) 1444–1451.
[6] C.A. Johnson, S. Brandenberger, P. Baccini, Acid neutralizing capacity of municipal waste incinerator bottom ash, Environ. Sci. Technol. 29 (1995) 142–147.
[7] C. Zevenbergen, L.P. Van Reeuwijk, J.P. Bradley, P. Bloemen, R.N.J. Comans, Mechanism and conditions of clay formation during natural weathering of MSWI bottom ash, Clays Clay Miner. 44 (4) (1996) 546–552.
[8] C. Zevenbergen, L.P. Van Reeuwijk, J.P. Bradley, R.N.J. Comans, R.D. Schuiling, Weathering of MSWI bottom ash with emphasis on the glassy constituents, J. Geochem. Explor. 62 (1998) 293–298.
[9] J.M. Chimenos, A.I. Fernández, R. Nadal, F. Espiell, Short-term natural weathering of MSWI bottom ash, J. Hazard. Mater. B79 (2000) 287–299.
[10] C. Speiser, T. Baumann, R. Niessner, Morphological and chemical characterization of calcium-hydrate phases formed in alternation process of deposited municipal solid waste incinerator bottom ash, Environ. Sci. Technol. 34 (2000) 5030–5037.
[11] C. Speiser, T. Baumann, R. Niessner, Characterization of municipal solid waste incineration (MSWI) bottom ash by scanning electron microscopy and quantitative energy dispersive X-ray microanalysis (SEM–EDX), Fresenius J. Anal. Chem. 370 (2001) 752–759.
[12] P. Piantone, F. Bodénan, L. Chatelet-Snidaro, Mineralogical study of secondary mineral phases from weathered MSWI bottom ash: implication for the modeling and trapping of heavy metals, Appl. Geochem. 19 (2004) 1891–1904.
[13] J.D. Eusden, T.T. Eighmy, K. Hockert, E. Holland, K. Marsella, Petrogenesis of municipal solid waste combustion bottom ash, Appl. Geochem. 14 (1999) 1073–1091.
[14] S. Sakai, M. Hiraoka, Municipal solid waste incinerator residue recycling by thermal processes, Waste Manage. 20 (2000) 249–258.
[15] O. Font, N. Moreno, X. Querol, M. Izquierdo, E. Alvarez, S. Diez, J. Elvira, D. Antenucci, H. Nugteren, F. Plana, A. López, P. Coca, F.G. Peña, X-ray powder diffraction-based method for the determination of the glass content and mineralogy of coal (co)-combustion fly ashes, Fuel 89 (2010) 2971–2976.
[16] A. Saffarzadeh, T. Shimaoka, Y. Motomura, K. Watanabe, Petrogenetic characteristics of molten slag from pyrolysis/melting treatment of MSW, Waste Manage. 29 (2009) 1103–1113.
[17] A. Saffarzadeh, T. Shimaoka, Y. Motomura, K. Watanabe, Chemical and mineralogical evaluation of slag products derived from the pyrolysis/melting treatment of MSW, Waste Manage. 26 (2006) 1443–1452.
[18] W.A. Deer, R.A. Howie, J. Zussman, An Introduction to the Rock-forming Minerals, Longman Group Limited, Hong Kong, 1992, p. 696.
[19] W.J.J. Huijgen, G.J. Ruijg, R.N.J. Comans, G.J. Witkamp, Energy consumption and net CO_2 sequestration of aqueous minerals carbonation, Ind. Eng. Chem. Res. 45 (2006) 9184–9194.
[20] N. Tanaka, Safely Construction and Management of Municipal Solid Waste Landfill, Gihodo Press, Tokyo, 2000, pp. 137–138.
[21] I.H. Thorseth, H. Furnes, O. Tumyr, A textural and chemical study of Icelandic palagonite of varied composition and its bearing on the mechanism of the glass–palagonite transformation, Geochim. Cosmochim. Acta 55 (1991) 731–749.
[22] R.A. Robie, B.S. Hemingway, J.R. Fisher, Thermodynamic Properties of Minerals and Related Substances at 298.15 K and 1 Bar (10^5 Pascals) Pressure and at Higher Temperatures, United States Government Printing Office, Washington, 1979, p. 456.
[23] K.B. Krauskopf, D.K. Bird, Introduction to Geochemistry, 2nd ed., McGraw-Hill, Inc., New York, 1979, pp. 464–477.
[24] S. Arickx, T. Van Gerven, E. Boydens, P. L'hoëst, B. Blanpain, C. Vandecasteele, Speciation of Cu in MSWI bottom ash and its relation to Cu leaching, Appl. Geochem. 23 (2008) 3642–3650.
[25] A. Saffarzadeh, T. Shimaoka, Y. Motomura, K. Watanabe, Characterization study of heavy metal-bearing phases in MSW slag, J. Hazard. Mater. 164 (2009) 829–834.
[26] J. Frolova, V. Ladygin, H. Franzson, O. Sigurðsson, V. Stefánsson, Petrophysical properties of fresh to mildly altered hyaloclasitite tuffs, in: Proceedings World Geothermal Congress, Antalya, Turkey, 24–29, April 2005, 2005.